

Article

Numerical and Analytical Determination of Steady-State Forces Acting on Cleats and Leads Conductor of the Power Transformer

Michał Smoliński^{1,2,*}  and Paweł Witzak² ¹ Hitachi Energy, 91-205 Lodz, Poland² Institute of Mechatronics and Information Systems, Lodz University of Technology, 90-924 Lodz, Poland; pawel.witzak@p.lodz.pl

* Correspondence: michal.smolinski@hitachienergy.com

Abstract: Electromagnetic forces acting on conductors of the cleats and lead of a power transformer can cause permanent damage to the insulation of conductors. Determining the force acting on the conductor of cleats and leads cannot be performed using the standard analytical formula because those conductors are in close proximity to the construction part of the active part made of ferromagnetic material. To calculate those forces in a steady state of a three-phase AC current, a parametric numerical simulation was conducted. Based on the simulation, a new analytical formula for forces acting on cables near the ferromagnetic plate was proposed by the authors. It was also noted that the presence of the ferromagnetic plate can increase the forces up to 60% compared to the same geometry without the plate. This publication also discusses how eddy currents and the proximity effect influence forces acting on conductors.

Keywords: electromagnetic forces; cleats and leads; power transformer; numerical simulation



Citation: Smoliński, M.; Witzak, P. Numerical and Analytical Determination of Steady-State Forces Acting on Cleats and Leads Conductor of the Power Transformer. *Energies* **2023**, *16*, 3600. <https://doi.org/10.3390/en16083600>

Academic Editors: José Antonio Domínguez-Navarro and Marco Merlo

Received: 13 March 2023

Revised: 10 April 2023

Accepted: 12 April 2023

Published: 21 April 2023



Copyright: © 2023 by the authors. Licensee MDPI, Basel, Switzerland. This article is an open access article distributed under the terms and conditions of the Creative Commons Attribution (CC BY) license (<https://creativecommons.org/licenses/by/4.0/>).

1. Introduction

In the three-phase power transformer, the electromagnetic forces acting on cleats and leads (C&L) conductors can be enormous. Especially in the case of an operational short circuit of power transformers with tertiary winding with a reduced power, the current density in C&L may reach the value of 280 A/mm^2 , which gives a peak phase current of approximately 100 kA, as in the case of the power transformer shown in Figure 1. The damage of the insulation of the cables in this transformer after the short circuit test is shown in Figure 1. This figure depicts three cables from three different phases near the core press plate. The insulation of those cables was destroyed near the supporting ribs due to the oscillation of cables during the short circuit test. This kind of failure is very difficult to predict during the design phase of a power transformer. To prevent the failure of insulation, the electromagnetic forces acting on the cables must first be known. Because cables are close to the core press plate, which is made of ferromagnetic material, forces acting on the cables cannot be determined by using an analytical formula. These forces can be determined by using magnetic stimulation. After knowing the force acting on cables, dynamic mechanical simulation must be conducted to simulate the oscillation of cables, and some failure criteria for insulation must be proposed. Building such a complex multiphysics model is time-consuming and much knowledge is needed. As each power transformer is designed individually according to customer needs, the cleats and leads designer does not have enough time to perform such a time-consuming algorithm. The idea of this publication was to develop analytical formulas that will approximate forces acting on conductors in the steady state of AC current. Having such analytical formulas helps the designer to calculate forces very quickly without using magnetic numerical simulation. This paper will not discuss the mechanical part of the problem. The mechanical model of the cable is awaited in further research.



Figure 1. Damaged insulation during short circuit test.

There is a very limited number of publications about forces acting on C&L conductors. However, there is a great number of papers focusing on short-circuit forces acting on the windings, and some of them will be described here. To determine short-circuit forces in windings, three main methods were used: numerical simulation, analytical formulas, and experiments. In ref. [1], a finite element method (FEM) simulation was used to calculate the electromagnetic field in the core and windings and determine forces during short-circuit and inrush conditions. The authors prepared two-dimensional and three-dimensional models of windings and compared axial and radial forces obtained from both simulations. The main conclusion was that there was a significant difference between forces calculated by 3D and 2D simulations. The radial force in the case of the 2D simulation was underestimated. In ref. [2], a magnetostatic analysis of the winding conductor was used to calculate the peak value of the force acting on windings. The peak forces calculated by the magnetostatic analysis were transferred to a static mechanical simulation to calculate the maximum deformation of the winding and determine its mechanical stiffness. Based on this coupled simulation, the critical buckling load for transformer winding was determined. The authors also prepared an experimental stand and measured the force in the short-circuit state and confirmed that the critical buckling load from the simulation differs by only 2.3% from the critical value obtained from the experiment. This publication shows how effective a good FEM method for the multiphysics system can be. Publication [3] presents a full dynamic multiphysics model of windings. The authors used a 2D transient simulation to calculate the dynamic electromagnetic forces acting on windings during the short circuit. The authors developed a mechanical model of windings and applied calculated forces from electromagnetic simulation to those windings. Based on a transient mechanical simulation, the deformation in winding and stresses in conductors as a function of time was determined. A similar approach of a multiphysics dynamic simulation was used in ref. [4] and ref. [5]; however, here, both the electromagnetic simulation and mechanical simulation were made using 3D transient solvers in COMSOL software.

Based on the presented publications, it can be concluded that using a multiphysics model to calculate forces acting on winding conductors and the mechanical response is widely used. However, building such a model is time-consuming. Therefore, an analytical approach to calculating forces is needed. Analytical formulas for radial and axial short-circuit forces were developed in ref. [6] and compared to results from numerical simulations. The results of the numerical simulation are in good agreement with the analytical formulas presented by the authors.

This paper concentrates on forces acting on the C&L of the power transformer. The authors found some selected publications discussing the geometry of straight conductors, which are similar to the problem in this paper. In ref. [7], a geometry consisting of three parallel busbars was analyzed. The forces acting on the busbars were calculated using the

analytical formula. A mechanical transient simulation was conducted to determine the deformation and mechanical stresses in the busbar. It should be mentioned that the use of analytical formulas to determine the forces was possible because the geometry was simple and there was no ferromagnetic material near the conductor, which is not the case with the system described in Figure 1. In ref. [8], a full multiphysics numerical model concerning electromagnetic, thermal, and mechanical phenomena was discussed. Based on this model, the dynamic deformation and equivalent stresses in busbars caused by electromagnetic forces and thermal effects were determined.

Comparing ref. [9], which presents the classical approach to modeling of short circuit state of power transformers to the more up-to-date refs. [10,11], it can be concluded that the requirements for modeling of the short circuit state operation of power transformers have significantly increased and currently numerical simulations are used more frequently to better model physics of short circuit state.

The discussed problem of the failure of the insulation is very complex because it involves both electromagnetic and mechanical phenomena. In order to fully solve the discussed problem, a multiphysics simulation is needed, consisting of an electromagnetic simulation and mechanical simulation. This paper focuses only on determining forces acting on the conductors of the cleats and leads of a power transformer. The mechanical modeling of a cleats and leads conductor is in progress and will be discussed in the next paper. As the conductor of cleats and leads consists of hundreds of small copper wires wound helically and insulation wrapped around the copper part, the mechanical modeling of such a system by the use of a numerical simulation is very difficult. Due to the complex geometry of the cables, the system is highly nonlinear, and force cannot be applied by one step, but by gradually increasing the force, which makes a mechanical simulation very difficult and time-consuming. Moreover, in this publication, the authors did not concentrate on the modeling of one case of a power transformer or a few cases, but rather developed a general approach on how to determine forces acting on cleats and leads conductors, analyzing the results from thousands of design points from parametric simulations and analytical formulas.

In Section 2, the analytical formula for forces acting on the cleats and leads conductors in a standard three-phase system without a ferromagnetic plate is determined. In Section 3, the authors describe the methods and results of the parametric numerical simulation of a magnetic field, concentrating on calculating forces acting on mentioned conductors. Firstly, the case without a ferromagnetic plate is discussed, and the results of the simulation are compared to the analytical equation from Section 2. As the next step, a number of parametric simulations with geometry consisting of three cables and a magnetic plate are presented. The forces determined by the numerical simulation were compared to the standard analytical formula from Section 2. In Section 3, the influence of geometrical parameters, as well as eddy currents in plate and cables, on forces acting on conductors is discussed. Based on parametric numerical simulations, the authors checked which parameters have a significant influence on the forces acting on the conductors and developed new improved formulas for forces acting on conductors near a ferromagnetic conductive plate, which are discussed in Section 4. In Section 5, all conclusions from the whole publication are presented.

2. Analytical Formulas for AC Forces in Steady State without the Ferromagnetic Plate

Before discussing a more advanced analysis, the theoretical formula for forces acting on cables in the symmetric three-phase in-plane system shown in Figure 2a will be discussed. The geometry mentioned in Figure 2a does not contain ferromagnetic plates, so simple analytical formulas can be discussed. The following assumptions were made for this analysis:

- The conductor is very long, so it can be assumed that the magnetic field is constant across the whole length of the conductor.
- The diameter of the cable is small with respect to the distance between cables.

- The currents flowing through cables are sinusoidal changing with angular frequency ω . The steady state is analyzed here. The phase of currents in cables 1, 2, and 3 are, respectively, 0, 120, and 240 degrees.

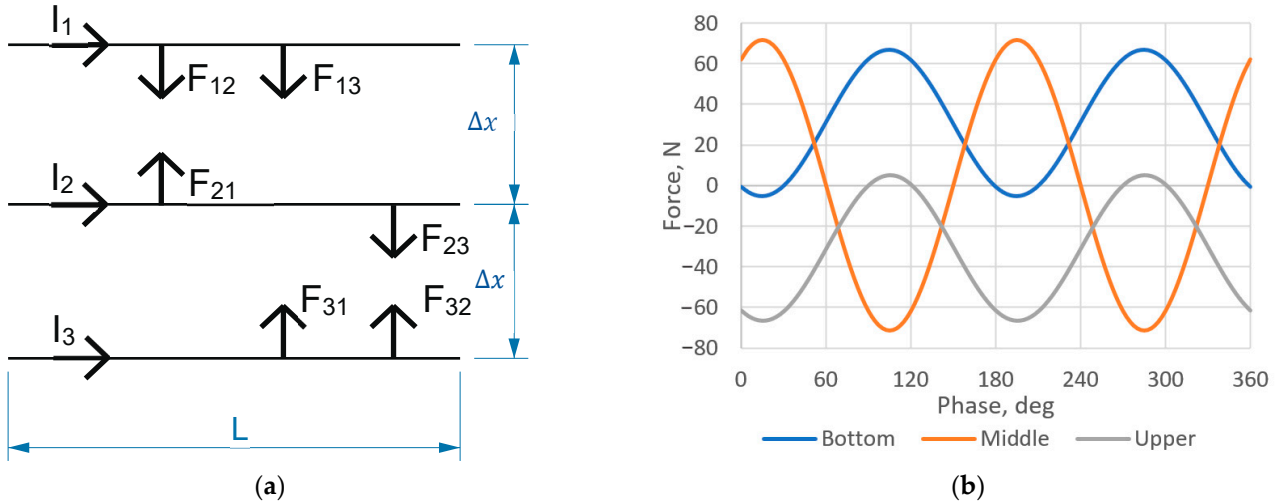


Figure 2. (a) Forces acting on 3 parallel conductors; (b) instantaneous forces acting on plane, 200 mm long system of three-phase conductors in air shifting each other by 60 mm and carrying 10 kA peak current.

Combining the Lorentz equation and Ampere law, the classic form of the instantaneous force $f_{km}(t)$ per unit length between two parallel conductors shifted by distance Δx and carrying the currents $i_m(t)$ and $i_k(t)$ holds [12]:

$$f_{km}(t) = \frac{\mu_0}{2\pi\Delta x} i_m(t) i_k(t) \tag{1}$$

The currents are symmetrically shifted in time but the set of conductors is not symmetric in space. We may distinguish the “middle” and two “side” conductors. The resultant force acting on the k -th conductor $f_k(t)$ is the sum of interactions with the remaining two.

$$f_k(t) = f_{km}(t) + f_{kn}(t) \tag{2}$$

It can be decomposed into two components: the constant in time F_{kDC} and alternating in time with the doubled network frequency 2ω and amplitude F_{kAC} .

$$f_k(t) = F_{kDC} + F_{kAC} e^{j(2\omega t + \varphi_k)} \tag{3}$$

The phase angles φ_k amount to 0 and $\pm 2\pi/3$. These amplitudes are obtained after simple trigonometric manipulations inserting sinusoidal relationships for phase currents. Their values are presented in Table 1 following the compact formula using the factor k . I stands for the amplitude of the AC current and the peak force F amounts to

$$F = k \frac{\mu_0}{\pi\Delta x} I^2 \tag{4}$$

Table 1. Values of factor k for set of three conductors supplied from three-phase network; subscripts are as in Figure 2a.

Force Component	F_{1DC}	F_{1AC}	F_{2DC}	F_{2AC}	F_{3DC}	F_{3AC}
k	$\frac{3}{16}$	$\frac{\sqrt{3}}{8}$	0	$\frac{\sqrt{3}}{4}$	$\frac{3}{16}$	$\frac{\sqrt{3}}{8}$

3. Numerical Simulations

The main goal of this publication was to study the forces acting on a three-phase system of cables situated close to the active part of the power transformer and carrying sinusoidal currents. This system is usually located near the ferromagnetic plate pressing the core as is shown in Figure 1. The said plate is made of a conductive, ferromagnetic material and, as will be described later, its presence has a great influence on the forces acting on the cables. Therefore, the analytical Equation (4) cannot be used directly. In order to calculate forces acting on the conductors, a numerical simulation must be applied.

The numerical simulation was conducted in ANSYS Maxwell 2021 R1 software in the eddy current module. This solver assumes that all quantities, such as the current density and magnetic field density, are sinusoidal changing with a defined frequency, so it only calculates the steady state of the AC current. The mentioned solver numerically solves the Maxwell equations in the form presented below [12].

$$\nabla \cdot D = \frac{\rho_e}{\epsilon_0} \quad (5)$$

$$\nabla \times E = -j\omega B \quad (6)$$

$$\nabla \cdot B = 0 \quad (7)$$

$$\nabla \times H = J + j\omega D \quad (8)$$

As a next step, the instantaneous force acting on each conductor was calculated by integrating Equation (9) over the volume of the cable [12].

$$F(t) = \int J(t) \times B(t) dV \quad (9)$$

Firstly, a parametric model consisting of three parallel cables supported by wooden brackets near the ferromagnetic plate was created. (Figure 3a) The presented parametric geometry is very close to the real geometry shown in Figure 1. By modifying the parameters (d , Δx , Δy , L , H , h), the geometry of the model can be changed and the influence of geometrical parameters on the force acting on the conductors can be investigated. The boundary condition assigned to all external surfaces of the model is a magnetic field tangent. As the excitation, the total current flowing through the cross-section of the cable was assigned to be the AC with amplitude I .

In the first simulation, the plate was omitted and eddy currents in cables were neglected. The instantaneous forces acting on cables obtained from the simulation are shown in Figure 2b. The force acting on the upper and bottom conductor consists of an AC component of 2ω frequency and a DC component, whereas, for the middle conductor, only the AC component is present. This is exactly as discussed in Section 2. Moreover, the numerical values of the DC force and AC force amplitude from theoretical Equation (4) are the same as those calculated by Maxwell software. This consistency in results between the simulation and theoretical formulas confirms that the simulation model is correct.

In order to investigate the influence of the plate on forces, a simulation with a plate made of ferromagnetic material with constant relative permeability $\mu_r = 290$ was conducted. Linear B-H characteristics were used to improve the speed of the simulation. The selected value of relative permeability was chosen according to the authors' experience. The results of selected linear simulations were compared to the simulation with nonlinear characteristics, and the difference between those results was considerably low. Four different simulations were carried out for the same geometry to investigate the influence of eddy currents in the plate and conductors on forces acting on the cables. In the first simulation, the plate was assumed to be nonconductive, and the conductors were stranded (eddy currents were neglected). The forces acting on the cable in the x -direction are shown in

Figure 4a. Comparing forces acting on cables near a non-conductive plate (Figure 4a) to forces acting on the conductor when the plate is not present (Figure 2b), it can be observed that the amplitude of forces is 25% higher when the plate is present. The force acting on the cables close to the nonconductive plate in the y-direction is shown in Figure 4b. In the case of simulation without the plate, the force in the y-direction is zero. From those simulations, two main conclusions can be drawn. Firstly, adding a ferromagnetic plate increases the magnitude of the force in the x-direction. Secondly, when the plate is present, a new component of force in the y-direction is present. This finally confirms that using the standard analytical Equation (4) is not enough because it will underestimate the forces.

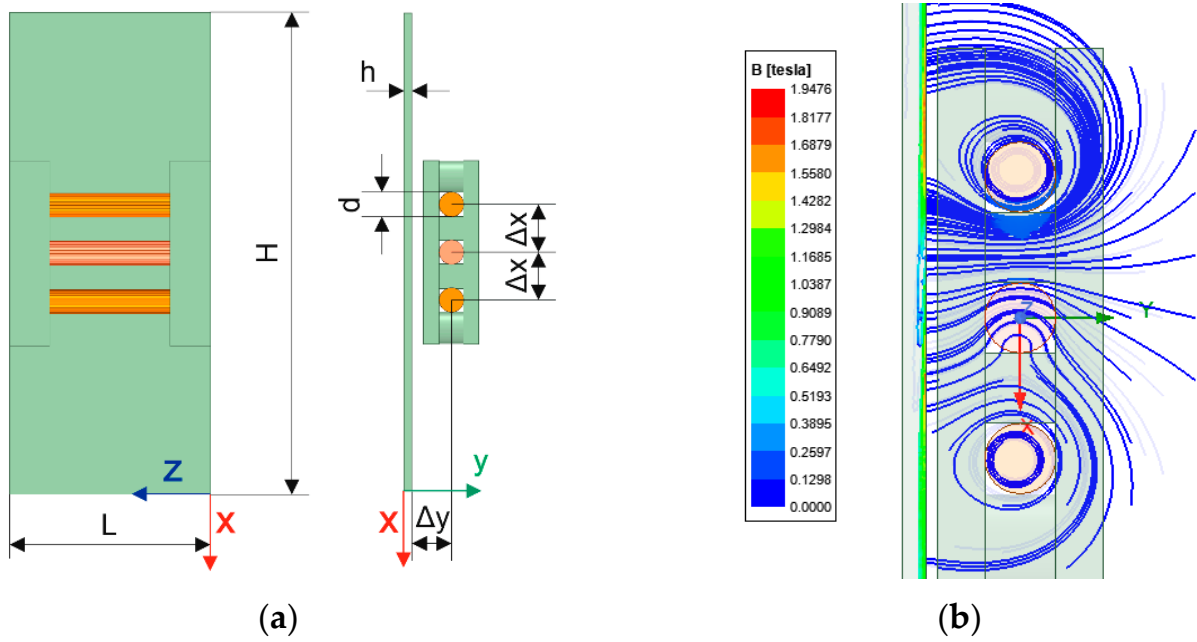


Figure 3. (a) Model of 3 cables near magnetic plate in ANSYS Maxwell; (b) magnetic flux density for simulation with conductive plate.

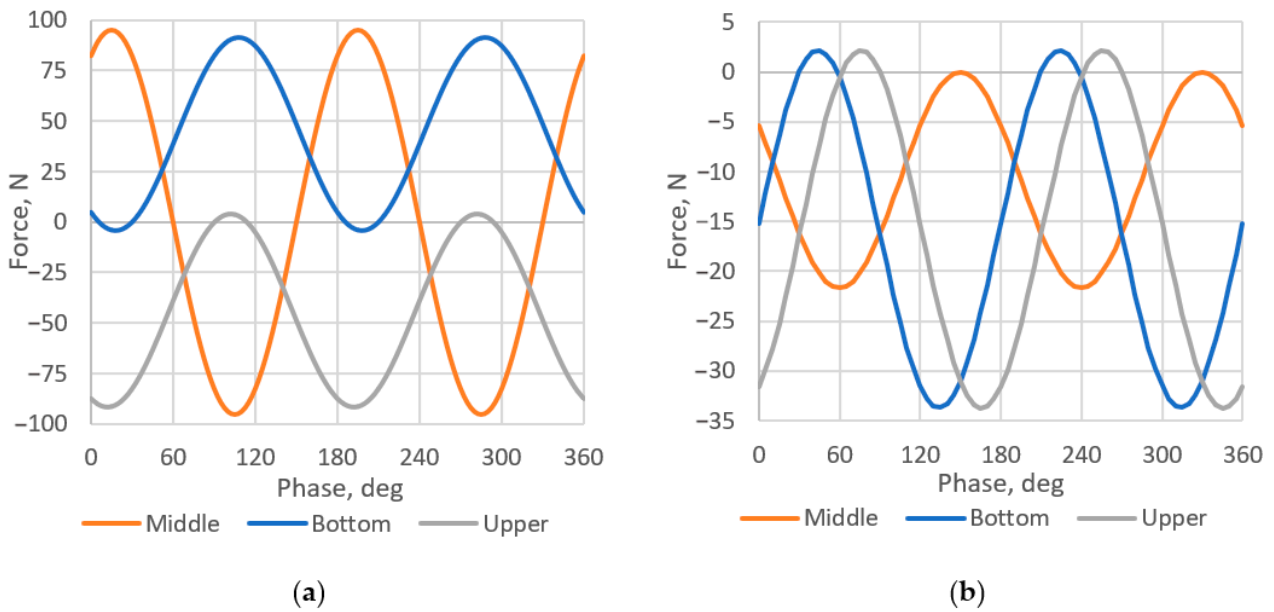


Figure 4. Instantaneous forces acting on stranded cables near a non-conductive core plate in (a) x direction; (b) y direction ($d = 30$ mm, $L = 200$ mm, $\Delta x = 60$ mm, $\Delta y = 40$, $H = 600$ mm, $I = 10$ kA).

In the second simulation, the eddy currents in plates were added, but eddy currents in cables were neglected. The assumed conductivity of the plate was 6.7×10^6 S/m. The graphs of instantaneous forces are very similar to those shown in Figure 4, so they will be omitted. After adding eddy currents to the plate, the force in the x -direction is lower than when eddy currents were not included in the model. Moreover, the induced eddy currents in the plate caused a nonzero DC force acting on the middle conductor, which was not the case for simulations without eddy currents.

In the third simulation, only eddy currents in the cable were activated and the plate was non-conductive. In this case, the DC force for the middle conductor was again nonzero. This clearly shows that adding the eddy currents either in cables or in the plate causes the DC force in the middle conductor and that the system is unsymmetric (the amplitudes of forces acting on the upper and lower conductor are also not the same). Moreover, the AC component of force is bigger if eddy currents are present in cables. In the last simulation, both currents in the cable and plate were taken into consideration, and the superposition of effects discussed earlier was present in this case.

In order to investigate the influence of geometrical parameters such as the distance between cables Δx or distance between cables and plate Δy on forces, a parametric simulation for each of the previously mentioned simulations was conducted. In order to better analyze the results, the forces acting on cables without a plate calculated by analytical Formula (4) were treated as the reference and the correction factors were defined to better visualize the influence of the ferromagnetic plate and eddy currents in cables and in the plate. The correction factors for the AC and DC force for the bottom and upper conductor and AC force for the middle conductor, given in Equations (10) and (11), can be used. The mentioned correction factors define the ratio of the force when the plate is present to the force obtained from the analytical formula. The same concept of the correction factor cannot be used for the DC force of the middle conductor, so the correction factor for the DC force for the middle conductor is defined, according to (12), as the ratio of the DC force with a plate to the AC force according to the analytical formula. As the forces in the y direction are significantly lower than in the x direction, they are not discussed in such detail.

$$k_{AC} = \frac{F_{AC \text{ wit cor plate}}}{F_A \text{ without cor plate}} \quad (10)$$

$$k_{DC} = \frac{F_{DC \text{ wit cor plate}}}{F_D \text{ without cor plate}} \quad (11)$$

$$k_{DC \text{ middle}} = \frac{F_{D \text{ middle wit cor plate}}}{F_{A \text{ middle without cor plate}}} \quad (12)$$

Now, the results of the mentioned parametric simulation will be discussed using corrections factors. Analyzing Figure 5a,b, it can be concluded that adding a plate always increases the force acting on the bottom conductor. The increase in force is bigger when the cables are very close to the ferromagnetic plate. Secondly, adding the eddy currents in plates always decrease the force in the bottom cable. However, adding the eddy current in the cables increases the force in the bottom cable. As can be seen, the increase in the force may reach 60% for the AC component and 40% for the DC component. This clearly shows that the influence of ferromagnetic plates and eddy currents in cables should not be neglected during the design process.

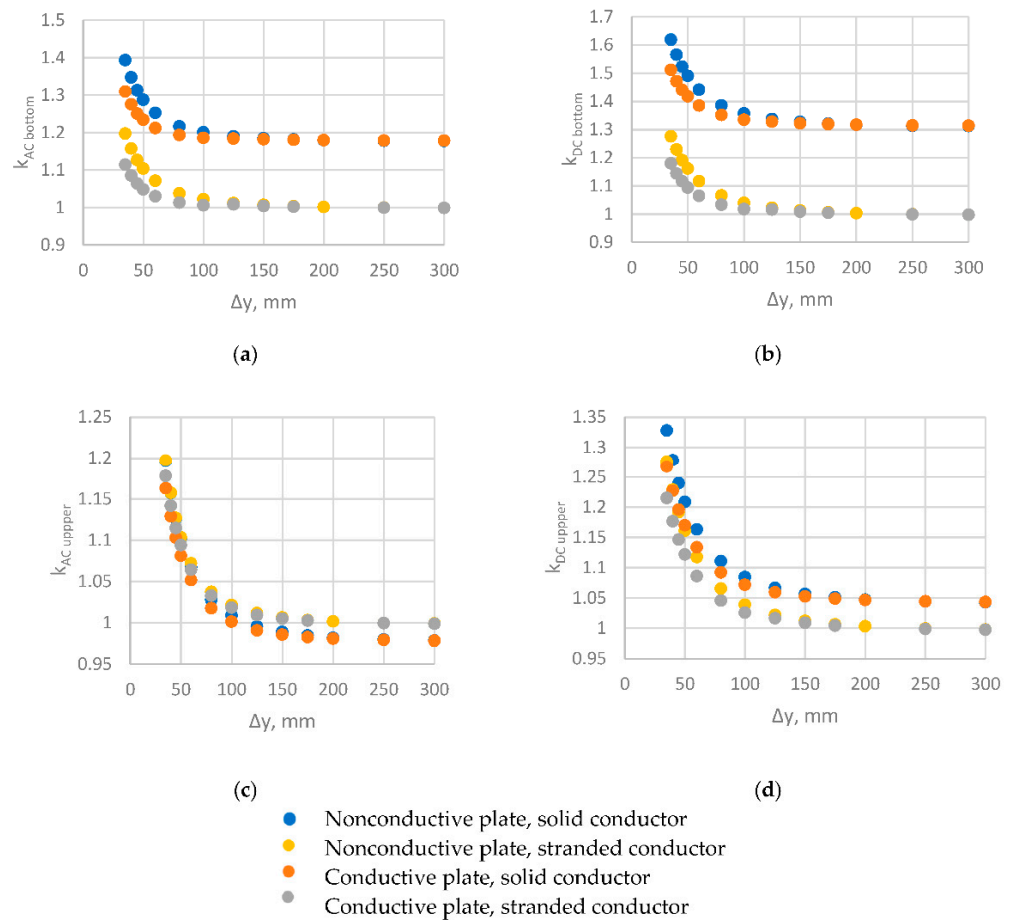


Figure 5. Correction factors: (a) $k_{AC\ bottom}$; (b) $k_{DC\ bottom}$ (c) $k_{AC\ upper}$; (d) $k_{DC\ upper}$ for $\Delta x = 35$ as a function of core plate distance.

Analyzing Figure 5c,d, it can be concluded that the forces acting on the upper conductor are lower than the forces acting on the bottom conductor (Figure 5a,b) if eddy currents are included either in cables or in the plate. This means that the eddy currents make the system unsymmetric. Similarly, as for the lower conductor, the eddy currents in the plate decrease forces acting on the upper conductor, and eddy currents in cables increase the forces acting on the upper conductor. This asymmetry depends on different phases of currents in bottom and upper conductors, and not on the geometry of the system.

The same conclusions can be drawn for the AC force acting on the middle conductor based on Figure 6a. Eddy currents in the plate decrease the AC force acting on the middle conductor, and eddy currents in conductors increase this force. Figure 6b–d show the correction factor for the DC force acting on the middle conductor for different distances between cables (35, 50, and 100 mm, respectively). In the case where eddy currents are neglected both in the plate and conductors, the DC component is zero. After adding conductivity to the plate, this force is nonzero due to eddy currents in the plate. Similarly, in the case of a solid conductor near a non-conductive plate, the force is also nonzero due to eddy currents in cables. However, the direction of force caused by eddy currents in a conductor is opposite to the direction of force caused by eddy currents in the ferromagnetic plate. This cannot be seen in the graphs below because those graphs only analyze absolute values of forces. Finally, after adding the eddy currents in both the conductor and plate, the superposition of both forces exists. As the directions of the forces are opposite, the values of the forces are subtracted. The component of the force coming from eddy currents in the conductor mainly depends on the distance between conductors and the diameter of the conductor. The closer the conductors are to each other, the more important this force is. On the other side, the force caused by eddy currents in the ferromagnetic plate is strongly

dependent on the distance between cables and the plate. The closer the cables are to the plate, the higher this force is. As a result, depending on the geometry, either the force caused by eddy currents in cables or the force caused by eddy currents in plates is higher, which can be seen in Figure 6b–d.

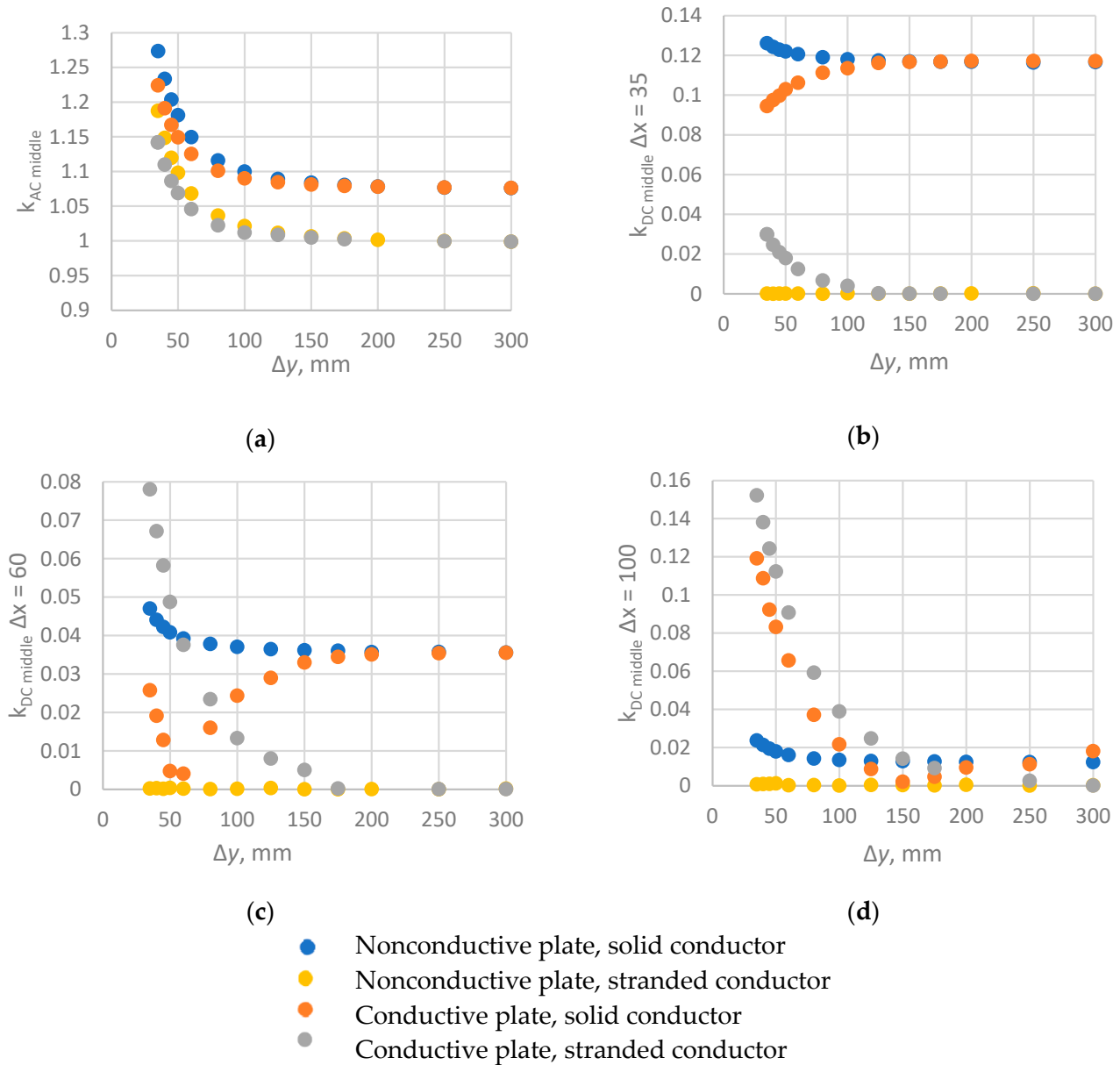


Figure 6. Correction factors: (a) $k_{AC\ middle}$ for $\Delta x = 35$; (b) $k_{DC\ middle}$ for $\Delta x = 35$; (c) $k_{DC\ middle}$ for $\Delta x = 60$; (d) $k_{DC\ middle}$ for $\Delta x = 100$; as a function of core plate distance.

In the previous simulation, the diameter of the cable was assumed to be 30 mm. However, eddy currents in cables strongly depend on the diameter of the cable and the distance between the conductors. For this reason, a parametric simulation with the diameter of the cable changing from 10 to 30 mm and the distance between cables changing from 35 mm to 300 mm was performed. Figure 7a presents the ratio of the AC force acting on the bottom solid conductor to the AC force acting on the stranded one for different values of the diameter of the cable and the distance between cables. This figure clearly shows that the influence of eddy currents is more significant for a large diameter of the cable and when cables are close to each other. This can be explained by the proximity effect. Due to the proximity effect, the magnetic field produced by one cable influences the current

distribution in the second cable. The smaller the distance between the cables, the bigger the influence of the magnetic field induced by one conductor in the other one. The bigger the diameter of the cable, the smaller the resistance of the cable, and eddy currents in the cable have higher values. In Figure 7b, the current density in the cable and the ferromagnetic plate is shown for phase angle 0. It can be seen that the current distribution is not uniform because one magnetic field of a neighboring conductor influences the current distribution in another one.

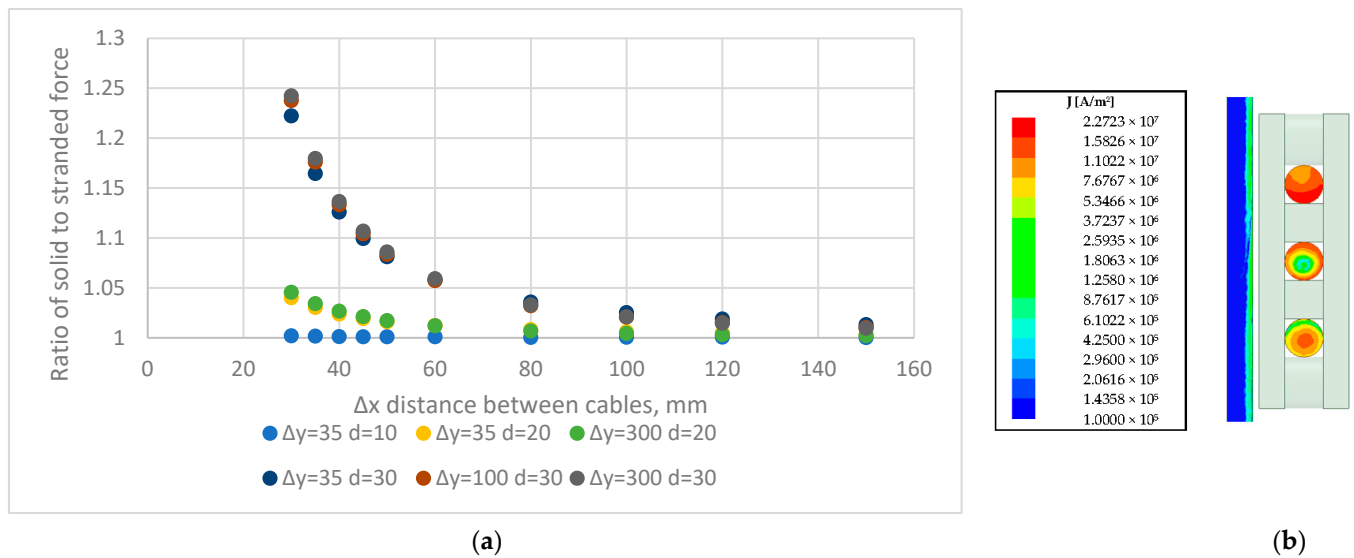


Figure 7. (a) Ratio of AC force acting on a solid conductor to force acting on stranded one for upper cable; (b) proximity effect for current density distribution.

The mentioned ratio of solid to stranded AC force for the bottom conductor can be approximated by Equation (13). A similar analysis was conducted for the other components of the force and the approximation functions will be described in the next section.

$$\frac{F_{x \text{ solid}}}{F_{x \text{ stranded}}} = 1 + C \frac{d^4}{\Delta x^2} \quad (13)$$

4. Improved Analytical Formulas

Based on all parametric simulations, analytical formulas are proposed approximating the forces acting on the cables near the conductive ferromagnetic plate. At the beginning, it was checked which parameters have a significant influence on the forces and which have negligible influence. The parameters with negligible influence (for example, the thickness of plate h) were not taken into consideration while developing improved formulas. The authors studied the influence of each parameter separately and the influence of a combination of parameters, trying to find the best mathematical function approximating the results of the simulations. After defining the proper mathematical formula, the least square method was used to determine the unknown constants in the equations.

Equations (14)–(16) can be used for three stranded cables near the conductive plate. The DC force for the middle conductor in the x -direction is described by Equation (16). All other forces in the x -direction are expressed by Equation (14). Equation (15) can be used to determine the forces in the y -direction.

$$F_{x \text{ stranded}} = \left(1 + A e^{-\alpha \frac{\Delta y}{\Delta x}}\right) k \frac{\mu_0 I^2 L}{\pi \Delta x} \quad (14)$$

$$F_{y \text{ stranded}} = B \frac{\mu_0 I^2 L}{\pi \Delta x} e^{-\beta \frac{\Delta y}{\Delta x}} \quad (15)$$

$$F_{x \text{ DC middle stranded}} = \left(A e^{-\alpha \frac{\Delta y}{\Delta x}} \right) k \frac{\mu_0 I^2 L}{\pi \Delta x} \tag{16}$$

Figure 8 presents the results from the simulation for different parameters and the approximation function. The maximum relative error of approximation is less than 5%, which is acceptable for engineering purposes.

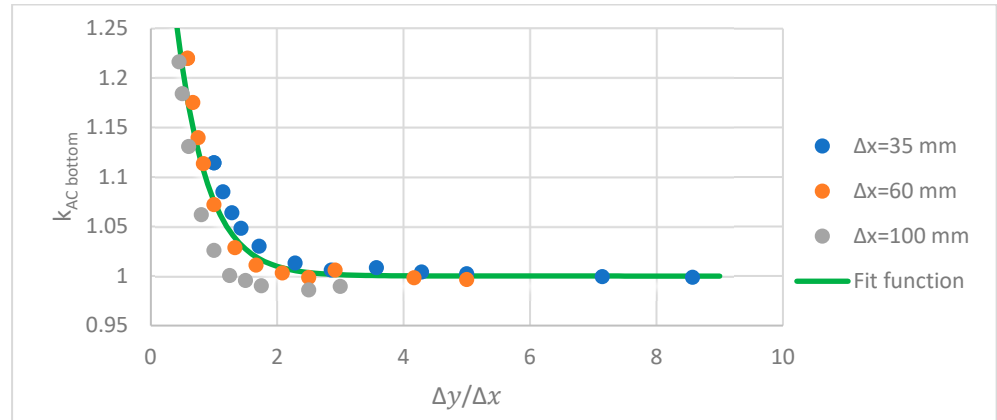


Figure 8. Simulation results and approximation function for stranded conductor.

The analytical formulas for forces acting on the solid cables near the conductive plate were determined and expressed by Equations (17)–(19). For all x -forces except for the DC force acting on the middle conductor, Equation (17) can be used.

$$F_{x \text{ solid}} = \left(1 + C \frac{d^4}{\Delta x^2} \right) \left(1 + A e^{-\alpha \frac{\Delta y}{\Delta x}} \right) k \frac{\mu_0 I^2 L}{\pi \Delta x} \tag{17}$$

For the DC component of the force acting on the middle conductor, Equation (18) must be used:

$$F_{x \text{ DC middle solid}} = \left| C \frac{d^4}{\Delta x^2} - A e^{-\alpha \frac{\Delta y}{\Delta x}} \right| k \frac{\mu_0 I^2 L}{\pi \Delta x} \tag{18}$$

For all y -forces, Equation (19) can be used.

$$F_{y \text{ solid}} = \left(1 + D \frac{d^4}{\Delta x^2} \right) B \frac{\mu_0 I^2 L}{\pi \Delta x} e^{-\beta \frac{\Delta y}{\Delta x}} \tag{19}$$

As it is depicted in Figure 9 the approximation function are with very good agreement to the results of simulations.

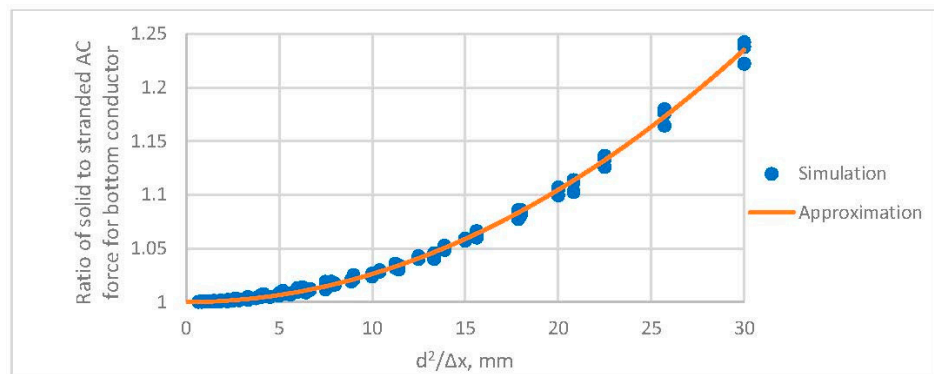


Figure 9. Simulation results and approximation function for solid conductor.

5. Conclusions

1. The electromagnetic forces acting on conductors of C&L can damage the insulation of the conductor. In order to prevent such a failure, it is necessary to know the forces acting on these conductors. Cables are very frequently in close proximity to ferromagnetic elements as core press plates, which makes the calculation of forces difficult.
2. In order to determine the forces acting on the conductor near ferromagnetic elements, the classical Equation (4) for long cables in a vacuum cannot be used because it will underestimate the forces acting on the conductors. Adding the ferromagnetic plate near to the cables causes an increase in the force acting on these cables in the direction parallel to the plate. The increase in force can be up to 60%, and it is stronger the closer the cables are to the plate.
3. Adding the ferromagnetic plate nearby the cable also causes the force in a direction perpendicular to the cables' plane. This force attracts cables toward the plate and it decreases when increasing the distance between the plate and cables. However, forces in the y -direction are always significantly smaller than forces in the x -direction.
4. The eddy currents in the ferromagnetic plate and cables significantly change the forces acting on the conductor. After adding eddy currents in the cables or the plate, the system is unsymmetric. The magnitude of the force acting on the upper and bottom conductor is different due to different phases of the current in those conductors. Furthermore, the eddy currents cause a nonzero DC force on the middle conductor.
5. Eddy currents in the plate cause a decrease in forces in the x -direction, except for the DC force acting on the middle conductor, which is nonzero, in contrast to the situation where eddy currents are neglected.
6. Eddy currents in cables increase the forces in the x -direction due to the proximity effect. The effect of eddy currents on forces increases when increasing the diameter of the cable and decreases when increasing the distance between two cables.
7. Based on the parametric simulation, new improved analytical formulas were developed to calculate forces acting on the cables near the ferromagnetic plate, which will be used in foreseen non-linear mechanical calculations of C&L set during operational short-circuit conditions.
8. Developing improved analytical equations is a big step forward for solving the problem discussed here. However, in order to use the mentioned equations in real engineering applications, a mechanical model of the conductor must be developed. Due to the complex geometry of cleats and leads conductors, performing the mechanical simulation is very difficult. Currently, the authors are in an advanced stage of developing the mechanical simulation, which will be described in the next paper.
9. In the future, experimental verification is foreseen by measuring the deflection of the realistic cable support geometry. This should be compared with the results from a complex non-linear numerical model of the structure, where the applied forces are given by the formulas given here. The finite element meshes in the electromagnetic and structural domains are completely different; therefore, the coupled magneto-mechanical approach cannot be used. A dynamic analysis of the structure seems to go beyond the scope of the presented work. The authors decided to trust the correctness of electromagnetic calculations, which were verified only for variants for which there is an analytical solution. The value added by this paper is the synthesis of thousands of finite elements solutions, showing the importance of several geometric dimensions influencing the final force value.

Author Contributions: Conceptualization, M.S. and P.W.; methodology, M.S. and P.W.; software, M.S.; validation, P.W.; formal analysis, P.W.; investigation, P.W.; resources, M.S. and P.W.; data curation, M.S.; writing—original draft preparation, M.S. and P.W.; writing: M.S. and P.W.; visualization, M.S.; project administration, P.W.; funding acquisition, P.W. All authors have read and agreed to the published version of the manuscript.

Funding: This research was funded by Technical University of Lodz.

Data Availability Statement: Not applicable.

Conflicts of Interest: The authors declare no conflict of interest.

References

1. Faiz, J.; Ebrahimi, B.M.; Noori, T. Three- and Two-Dimensional Finite-Element Computation of Inrush Current and Short-Circuit Electromagnetic Forces on Windings of a Three-Phase Core-Type Power Transformer. *IEEE Trans. Magn.* **2008**, *44*, 590–597. [[CrossRef](#)]
2. Geißler, D.; Leibfried, T. Short-Circuit Strength of Power Transformer Windings-Verification of Tests by a Finite Element Analysis-Based Model. *IEEE Trans. Power Deliv.* **2017**, *32*, 1705–1712.
3. Zhang, H.; Yang, B.; Xu, W.; Wang, S.; Wang, G.; Huangfu, Y.; Zhang, J. Dynamic Deformation Analysis of Power Transformer Windings in Short-Circuit Fault by FEM. *IEEE Trans. Appl. Supercond.* **2014**, *24*, 4. [[CrossRef](#)]
4. Zhou, D.; Li, Z.; Ke, C.; Yang, X.; Hao, Z. Simulation of transformer windings mechanical characteristics during the external short-circuit fault. In Proceedings of the 2015 5th International Conference on Electric Utility Deregulation and Restructuring and Power Technologies (DRPT), Changsha, China, 26–29 November 2015; pp. 1068–1073.
5. Yadav, S.; Mehta, R.K. FEM Based Study of Short Circuit Forces on Power Transformer Windings. In Proceedings of the 2019 3rd International Conference on Recent Developments in Control, Automation & Power Engineering (RDCAPE), Noida, India, 10–11 October 2019; pp. 540–544.
6. Ebrahimi, B.M.; Fereidunian, A.; Saffari, S.; Faiz, J. Analytical estimation of short circuit axial and radial forces on power transformers windings. *IET Gener. Transm. Distrib.* **2014**, *8*, 250–260. [[CrossRef](#)]
7. Szulborski, M.; Łapczyński, S.; Kolimas, Ł.; Kozarek, Ł.; Rasolomampionona, D.D. Calculations of Electrodynamics Forces in Three-Phase Asymmetric Busbar System with the Use of FEM. *Energies* **2020**, *13*, 5477. [[CrossRef](#)]
8. Kadkhodaei, G.; Sheshyekani, K.; Hamzeh, M.; Dadjo Tavakoli, S. Multiphysics analysis of busbars with various arrangements under short-circuit condition. *IET Electr. Syst. Transp.* **2016**, *6*, 250–260. [[CrossRef](#)]
9. Bertagnolli, G. *The ABB Approach to Short-Circuit Duty of Power Transformers*, 1st ed.; ABB Ltd.: Zurich, Switzerland, 1996.
10. Cuesto, M.; Porrero, J.; Munoz, M.; Camara, J.; Hurlet, P.; Tanguy, A.; Ryadi, M. *Short Circuit Design Conception and Validation of a 570 MVA, Single-Phase GSU-Transformer by SC-Withstand Tests on a Mock-Up Unit*; Cigre: Paris, France, 2016; A2-206.
11. Forslin, J.; Tillery, J.; Muñoz, M.; Saccone, D. *State of the Art in Short-Circuit for Transformers*; Cigre: Paris, France, 2022; A2-10506.
12. Griffiths, D.J. *Introduction to Electrodynamics*, 4th ed.; Cambridge University Press: Cambridge, UK, 2017.

Disclaimer/Publisher's Note: The statements, opinions and data contained in all publications are solely those of the individual author(s) and contributor(s) and not of MDPI and/or the editor(s). MDPI and/or the editor(s) disclaim responsibility for any injury to people or property resulting from any ideas, methods, instructions or products referred to in the content.